HAL
open science

A Tight-Binding Grand Canonical Monte Carlo Study of the Catalytic Growth of Carbon Nanotubes [Working paper]

Hakim Amara, Christophe Bichara, François Ducastelle

To cite this version:

Hakim Amara, Christophe Bichara, François Ducastelle. A Tight-Binding Grand Canonical Monte Carlo Study of the Catalytic Growth of Carbon Nanotubes [Working paper]. 2007. hal-00141874

HAL Id: hal-00141874

https://hal.science/hal-00141874v1

Preprint submitted on 16 Apr 2007

HAL is a multi-disciplinary open access archive for the deposit and dissemination of scientific research documents, whether they are published or not. The documents may come from teaching and research institutions in France or abroad, or from public or private research centers.

L'archive ouverte pluridisciplinaire **HAL**, est destinée au dépôt et à la diffusion de documents scientifiques de niveau recherche, publiés ou non, émanant des établissements d'enseignement et de recherche français ou étrangers, des laboratoires publics ou privés.

A Tight-Binding Grand Canonical Monte Carlo Study of the Catalytic Growth of Carbon Nanotubes

H. Amara,[1,2] C. Bichara,[3] and F. Ducastelle[4]

[1]*Laboratoire de Physique du Solide,*
Facultés Universitaires Notre-Dame de la Paix,
61 Rue de Bruxelles, 5000 Namur, Belgique

[2]*PCPM and CERMIN, Université Catholique de Louvain,*
Place Croix du Sud 1, 1348 Louvain-la Neuve, Belgique

[3]*CRMCN-CNRS, Campus de Luminy,*
Case 913, 13288 Marseille Cedex 09, France.

[4]*Laboratoire d'Etude des Microstructures,*
ONERA-CNRS, BP 72, 92322 Châtillon Cedex, France.

(Dated: April 16, 2007)

hal-00141874, version 1 - 16 Apr 2007

Abstract

The nucleation of carbon nanotubes on small nickel clusters is studied using a tight binding model coupled to grand canonical Monte Carlo simulations. This technique closely follows the conditions of the synthesis of carbon nanotubes by chemical vapor deposition. The possible formation of a carbon cap on the catalyst particle is studied as a function of the carbon chemical potential, for particles of different size, either crystalline or disordered. We show that these parameters strongly influence the structure of the cap/particle interface which in turn will have a strong effect on the control of the structure of the nanotube. In particular, we discuss the presence of carbon on surface or in subsurface layers.

PACS numbers: 68.55.Ac, 61.46.Fg, 82.65.+r

Accurately controlling the location, diameter, chirality and length of single wall carbon nanotubes elaborated by chemical vapor deposition (CVD) is one of the critical issues for an effective use of the unique properties of these nanoobjects in many applications such as electronic devices[1]. According to Nasibulin *et al.*[2] and Bachilo *et al.*,[3] the diameter of the tubes produced by CVD is related to the diameter of the catalyst particle from which they originate. One important step is therefore to control the size distribution and the location of the catalyst particle. Chirality may result from either thermodynamic stability differences between the initial tube caps[4] or from difference in the growth kinetics.[5] The tube length can be limited by the poisoning of the catalyst resulting from uncontrolled growth parameters.

The very large number of parameters controlling the CVD reaction makes it necessary to rationalize the approach by an understanding of nucleation and growth mechanisms at the atomic level. Experimental investigations at this level are usually done by Transmission Electron Microscopy (TEM) performed *post mortem* outside the CVD reactor. Remarkable progress has recently been made in the *in situ* observation of the growth of nanotubes,[6,7,8] but the atomic resolution is not obtained under the actual growth conditions.

Computer simulation techniques are an alternative way to gain an insight at the atomic level. However, they have to face the very difficult challenge of requiring an accurate description of the interatomic interactions, as typically provided by first principles calculations, and to address the size and time scales relevant to the experimental situation. Efficient catalyst particles for CVD reactions are in the 1–10 nm diameter range (some thousands of atoms) and, according to Lin *et al.*,[9] the time scale for the nucleation and growth of tubes is in the 10–100 seconds range. Such scales are largely beyond the capabilities of Molecular Dynamics (MD) techniques, even with the most simple interatomic interaction models. This means that only some elementary steps can be studied, or that the growth conditions imposed in the simulations are orders of magnitude too fast, resulting in very defective structures as compared to the almost perfect tubes obtained experimentally.

Static *ab initio* calculations have been used to calculate the total energies of atomic configurations considered as representative of the nucleation of carbon caps on a catalyst.[10]

Hofmann *et al.*[11] proposed a schematic growth model and calculated the relevant activation barriers. Abild-Pedersen *et al.*[12] showed that carbon surface or subsurface diffusion on Ni correspond to almost equal diffusion barriers. First principles Molecular Dynamics simulations were used to study the root incorporation of C atoms on a Co catalyst[13] and the nucleation of a carbon cap on a Fe droplet was described by Raty *et al.*.[14] As argued by these latter authors the absence of diffusion inside the Fe particle is due to its very small size (55 atoms). This is at odds with the findings of Ding and Bolton[15] who argued that highly supersaturated carbon concentrations are required for nucleating carbon islands on the Fe particle surface. This difference might be due to the FeC interaction (empirical versus *ab initio*) model used or to the very short physical time of the first principles simulations. The same group studied the roles of the particle size and of a possible temperature gradient on the nanotube growth.[16] Based on their empirical MD simulations, Shibuta and Maruyama[17] found hexagonal carbon networks formed within a small Ni cluster of 108 atoms, in complete contradiction with the *ab initio* calculations of Zhang *et al.*[18] showing that, at 0 K, the most stable position for one C atom on a small Ni_{38} hexagonal cluster is adsorbed on the surface rather than in the central interstitial site. Studying the growth of nanotubes on small (Ni_{48} and Ni_{80}) clusters by empirical MD, Zhao *et al.*[19] found almost the same mechanism as in our previous calculations on a semi infinite system (slab geometry)[20] based on a tight binding model. In both studies, four steps can be identified: C dissolution, the formation of C chains on the surface followed by the formation of sp^2 C sites that gradually detach from the catalyst surface.

Summarizing the computer simulations results, it seems that the question of the presence of carbon dissolved in the catalyst remains quite controversial. First principles static or dynamic calculations tend to show that no C is dissolved in the very small particles studied, while empirical simulations tend to find a larger amount of C dissolved. Besides the questions of the accuracy of the interatomic force model and of the time scale of the simulations, another aspect is completely neglected in the MD calculations used. Molecular Dynamics works by construction in a microcanonical or canonical ensemble with a fixed number of particles. Growth sequences are obtained either by adding particles "by hand" or by putting the catalyst particle in a box, with a fixed number of C atoms in a vapor phase. Such a process completely ignores the chemical potential gradient that is the

thermodynamic driving force for the growth.

In this paper, using a carefully tested tight binding model we show that the solubility of carbon and the possibility to grow tube embryos at the surface of small Ni cluster critically depend on the carbon chemical potential. Moreover, we show that, at 1000 K, the solubility of carbon also depends on the structure of the small metallic cluster considered : disordered, liquid-like clusters incorporate more C atoms, while they tend to remain adsorbed on the surface of crystalline structures.

The tight binding model we used for C and Ni interactions has already been used by Amara *et al.*[20] and is described in detail in reference 21. The total energy is taken as a sum of a band structure term and an empirical repulsive term. The s and p electrons of C and d electrons of Ni are included. Calculations are performed in the grand canonical ensemble, with fixed volume, temperature (T), number of Ni atoms and C chemical potential (μ_C). In order to be efficiently implemented in the grand canonical Monte Carlo (GCMC) code, the total energy has to be taken as a sum of local terms, avoiding to recalculate the total energy of the whole box at each step of the Monte Carlo process. This is achieved by calculating local densities of electronic states using the recursion method.[22] To keep the model as simple and fast to compute as possible, we neglect the Ni s electrons and calculate only the first four moments of the local densities of states. The local energy of each atom therefore depends only on the positions and chemical identities of its first and second neighbors, as defined by a cut off distance set at 3.20 Å for first neighbors.

The GCMC calculations presented here compare the adsorption of carbon atoms on small Ni clusters, either "crystalline", in their face centered cubic equilibrium Wulff shape, with 201, 405, or 807 atoms, or disordered, resulting from the quench of liquid droplets with 50 or 108 atoms. These calculations were done at 1000 K, a typical temperature for the CVD synthesis of single wall nanotubes. We analyze the influence of the carbon chemical potential on the carbon nanostructure grown on the Ni cluster, on the structure of the nickel carbon interface and on the solubility, if any, of carbon in the Ni cluster. The decomposition reaction of the carbon rich feedstock under specific partial pressure conditions is not taken into account explicitly in our calculations. However, the result of

this reaction is to provide atomic carbon with a given chemical potential that is able to adsorb and diffuse on, or in, the nickel surface. As explained in e.g. Lolli *et al.*,[5] this carbon chemical potential is experimentally controlled through the thermochemistry of the decomposition reaction. To achieve this in the computer experiments, we use Monte Carlo simulations in the grand canonical ensemble.[23]

The grand canonical algorithm used consists in a series of Monte Carlo macrosteps. Each macrostep randomly alternates displacement moves for Ni or C atoms, attempts to incorporate carbon in a previously defined active zone and attempts to remove existing carbon atoms. Within each macrostep, we systematically performed four times the number of atom attempted displacement steps. To incorporate carbon atoms in the structure, 1000 attempts were made and ended as soon as one successful incorporation has occurred. The number of attempted carbon removal steps was equal to twice the number of C atoms present in the structure. We typically performed up to 5000 macrosteps. We will see below that this number of macrosteps is large enough to reach equilibrium when the chemical potential conditions are such that no carbon nanostructure grows. Of course, under growth conditions, no equilibrium is ever reached and the number of adsorbed C atoms keeps increasing. The maximum amplitude of the attempted displacements of Ni or C atoms is adjusted during the run in order to have a rejection rate around 50%, ensuring an optimal use of the computer resources to sample the configurational space of the system.[23] On average, the maximum amplitude of the displacements of Ni atoms turns out to be twice as large as that of C atoms, meaning that the mobility of Ni atoms is larger. In order to mimic the CVD process, the active zone for inserting or extracting carbon atoms is defined as a region of space at less than 3 Å above and 3 Å below the surface of the Ni cluster. Moreover, to avoid the encapsulation of the Ni cluster with carbon and to account for the fact that, in the experiments, the catalytic particles are supported, the active zone is limited to the topmost (60%) part of the cluster. We stress that this is a very crude approximation that neglects the modifications of the cluster structure that can be induced by the substrate.[24] In the case of the largest fcc Wulff-shaped clusters, this zone is smaller: 50% for the 405 atoms cluster and 40% for the 807 atoms cluster. A first reason for this is to limit the CPU time of the calculations, since the fourth moment tight binding model for Ni and C atoms is replaced by a much simpler second moment approximation model for Ni

atoms only, as soon as they are far enough from any C atom (i. e.: at a distance larger than 6.4 Å). A second reason is that these fractions of the clusters volume roughly correspond to the same number of Ni atoms (151 for the 201 atom cluster, 231 for the 405 atoms one and 267 for the 807 atoms one), which will be used to calculate the mole fraction of carbon atoms dissolved in the Ni structure.

To analyze the results of the calculations, we will have to discriminate between carbon atoms that are outside the Ni cluster, generally forming *sp* (small chains) or sp^2 (layered) structures and individual carbon atoms that are adsorbed on the surface or incorporated in subsurface or bulk. A convenient way to do this is to calculate the distance between the carbon atom of interest and its nearest carbon neighbor. If this distance is smaller than 1.7 Å , the atom is defined as an "outer" C atom, because C–C bond lengths in *sp* or sp^2 bonding states are smaller than this. If it is longer, the carbon atom is either adsorbed on the Ni surface, with Ni neighbors in the 1.85–1.95 Å distance range, or incorporated in interstitial sites: such carbon atoms are denoted as "inner" carbon atoms in the following. This criterion stems from the analysis of the carbon carbon pair correlation function that clearly shows distinctive features for each type of atoms. It can be easily checked by a visual inspection of the structures formed.

We first study the effect of the carbon chemical potential on the structures formed outside the particle. Starting with the same Ni_{50} disordered droplet, we performed GCMC runs with μ_C varying between -6.00 and -4.50 eV/atom, by steps of 0.75 eV/atom. The carbon chemical potential is referred to a fictitious ideal monoatomic gas, explaining its values that are of the order of the cohesive energies of the various carbon phases (e.g.: -7.41 eV/atom for a graphene layer in our model). Figure 1 shows a series of typical configurations obtained under these conditions. At low chemical potential, no outer carbon structure is formed. Carbon atoms land on the surface and tend to diffuse on the surface or towards subsurface sites. They sometimes form carbon dimers, but no twofold coordinated long chain structure is ever formed. An equilibrium situation is quickly reached, with about 25 C atoms adsorbed. On the contrary, when the chemical potential is much larger (-4.5 eV/atom), a disordered and thick carbon layer is formed outside the cluster. This amorphous layer is formed by carbon atoms with 3 or 4 carbon neighbors. This can be

interpreted as the growth of an amorphous carbon fiber. A much more interesting situation, as far as the formation of a carbon nanotube is concerned, is observed at intermediate chemical potential values.

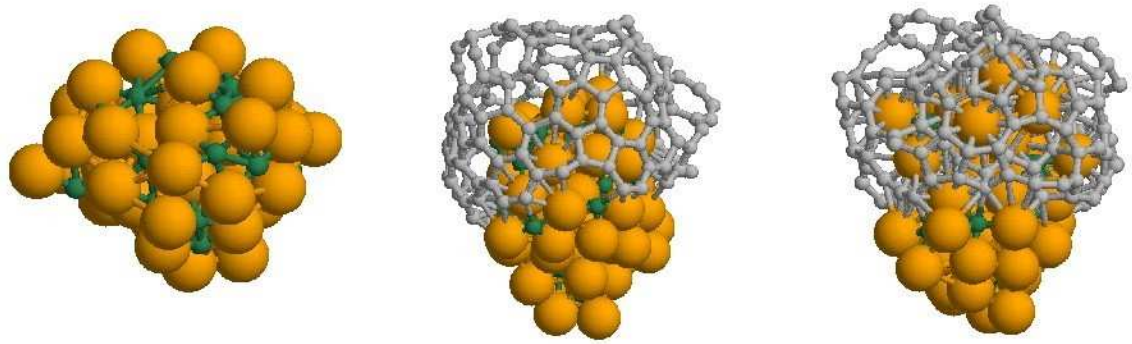

FIG. 1: Typical configurations resulting from GCMC simulations of the growth of C on a 50 Ni atom disordered droplet at 1000 K. Left panel, μ_C = -6.00eV/atom, central panel μ_C = -5.25 eV/atom, right panel μ_C = -4.50 eV/atom. 5000, 4000 and 2500 Monte Carlo macrosteps were performed, respectively. Nickel atoms are represented in orange, inner carbon atoms are in green and outer carbon atoms are in grey. See text for the definition of "inner" and "outer" carbon atoms.

At μ_C = -5.25 eV/atom and 1000 K, a cap of carbon atoms is formed. It encapsulates the topmost part of the Ni droplet. Figure 2 presents a series of configurations characteristic of the formation of the cap. At the very beginning of the GCMC run, carbon atoms "land" on the available surface of the Ni particle. Then, instead of diffusing towards subsurface sites as observed at lower chemical potentials, they tend to form dimers and short chains at the surface of the droplet. Because μ_C is larger, the flux of incoming atoms is larger and C atoms quickly find another C to form a C–C bond that stabilizes it on the surface. Although no time scale is included in the grand canonical Monte Carlo scheme, we can see that this step is very fast: in less than 50 Monte Carlo macrosteps, carbon chains are already formed on the surface. As observed in our previous calculations on Ni slabs,[20] the chains grow, cross each other to form threefold coordinated sp^2 carbon sites that act as nucleation centers to grow sp^2 layers. These sp^2 carbon atoms interact weakly with the Ni surface and the cap formed can gradually detach from the droplet. The difference with

calculations performed on flat surfaces is that the curvature of the Ni droplet induces a curvature of the carbon cap. The cap diameter and curvature are determined by the Ni particle shape at the moment when the cap is formed. However, since Ni atoms are more mobile than C atoms, the shape of the Ni droplet can be modified later in the process. As compared to the almost perfect graphene like layer, mostly formed with hexagons, obtained on a flat Ni surface, the curvature and growth conditions impose a larger number of defects such as pentagons, heptagons, etc. The cap structure shown in figure 1 is formed by 13 pentagons, 28 hexagons, 7 heptagons, 5 octogons and 7 9-membered rings. The cap is very defective as compared to ideal nanotube terminations that require only a small number of pentagons to be formed.[25] The larger number of defects observed here results from the growth conditions: the carbon chemical potential chosen to obtain realistic structures in a reasonable, although long, CPU time is probably too high. Under such conditions, the growth is too fast and the defects formed have a very small probability to be healed.

The GCMC calculations presented above indicate that there is an optimal carbon chemical potential to grow sp^2 carbon caps on a very small Ni droplet. When the carbon chemical potential is large enough, carbon nanostructures are formed outside the Ni droplet, while some carbon atoms remain adsorbed on the surface, in close contact with Ni atoms, or even diffuse inside the particle. The mole fraction of these inner C atoms depends on the carbon chemical potential and on the temperature, as indicated by comparing with our previous calculations at 1500 K.[20] We note here that it also depends on the particle size and on the structural state of the Ni cluster. In order to analyze these latter points, we performed the same calculations on a larger disordered droplet with 108 Ni atoms and on face centered cubic clusters with a truncated octahedron shape that minimizes their total (surface + volume) energy. These so called Wulff-shaped clusters have only (111) and (100) facets. Three sizes were considered: 201, 405 and 807 Ni atoms. At 1000 K and μ_C = -5.25 eV/atom, the results are qualitatively the same, as far as the cap formation is concerned. As shown in figure 3, more or less defective carbon layers are formed on the cluster surface. Their shape is imposed by the cluster geometry. In order to allow them to detach from the surface, much longer runs should be performed, as has been done for the Ni_{50} disordered cluster. It is interesting to notice that the crystalline structure of the cluster is preserved, although the Ni atoms on the edges are less stable than the others and can be strongly

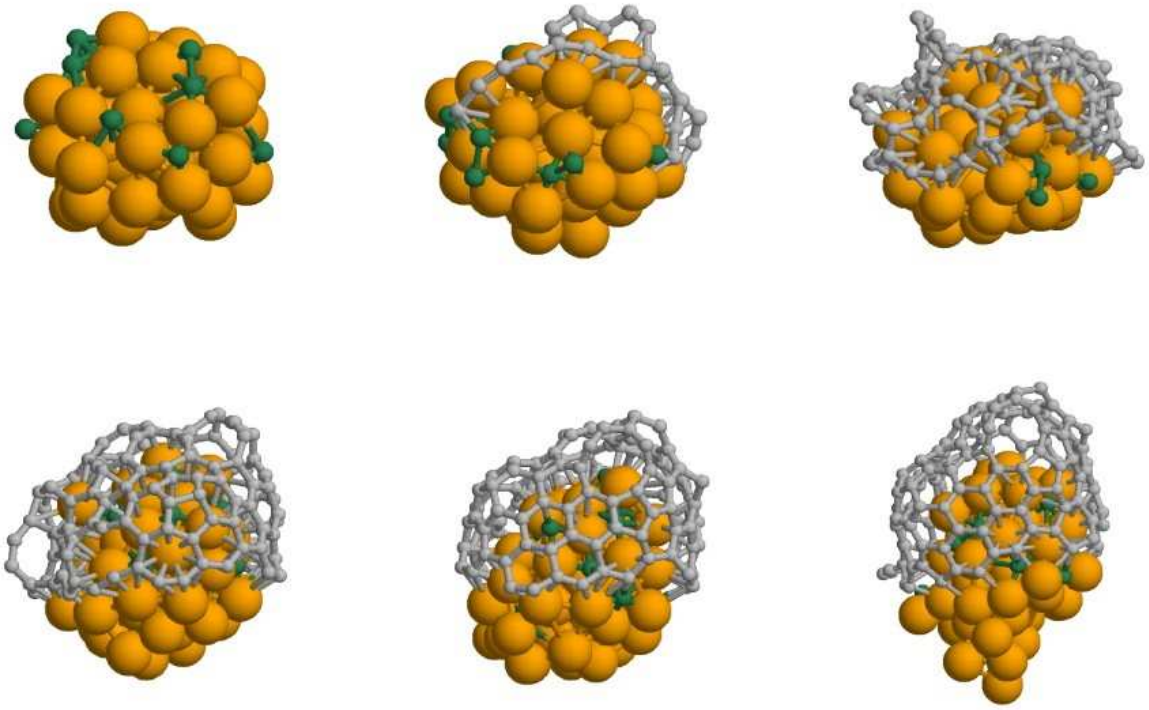

FIG. 2: Typical growth sequence during a GCMC simulation of the adsorption of C on a 50 Ni atom disordered droplet at 1000 K and μ_C = -5.25 eV/atom. From left to right and top to bottom: 1) carbon atoms or diatoms adsorbed; 2) chains growing; 3 and 4) cap formed; 5 and 6) cap detaches from the Ni droplet. Nickel atoms are represented in orange, inner carbon atoms are in green and outer carbon atoms are in grey. See text for the definition of "inner" and 'outer" carbon atoms.

displaced, as shown on the right hand image in figure 3.

A visual inspection of the structures obtained seems to indicate that the number of dissolved C atoms is smaller in the case of crystalline structures than in the disordered ones. This is confirmed by the analysis of the mole fraction of inner carbon atoms as a function of the number of Monte Carlo macrosteps, plotted in figures 4 and 5. For the disordered structures, the mole fraction of inner C atoms is calculated with respect to the total number of Ni atoms (respectively 50 and 108), because the particles are small and C atoms tend to diffuse in the whole structure. As mentioned above, for the fcc clusters, the mole fraction of inner C atoms is calculated with respect to a smaller number of Ni atoms. These different

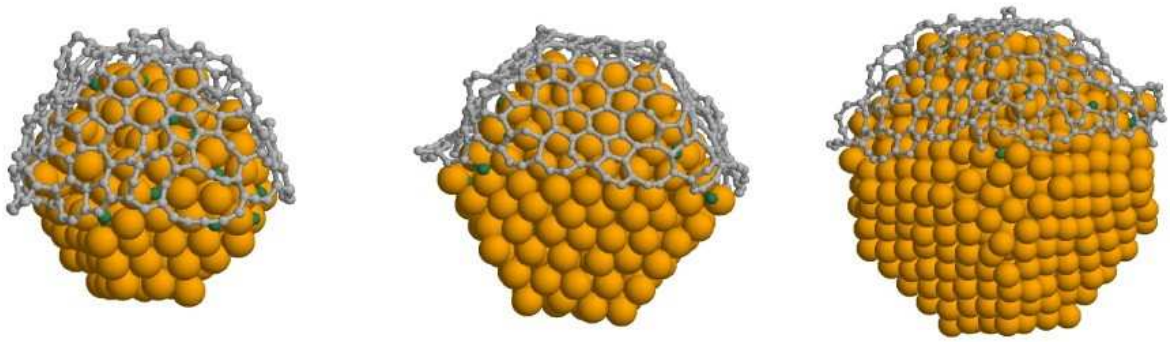

FIG. 3: Typical configurations resulting from GCMC simulations of the growth of C on nickel fcc Wulff-shaped clusters at 1000 K and μ_C = -5.25 eV/atom. Left: 201, center: 405 and right: 807 Ni atoms. The active zones for the GCMC calculations were the topmost 60%, 50% and 40% respectively (see text). Nickel atoms are represented in orange, "inner" carbon atoms are in green and "outer" carbon atoms are in grey. See text for the definition of "inner" and "outer" carbon atoms.

ways of calculating the mole fractions tend to minimize the differences between the carbon solubilities in crystalline or disordered clusters. At 1000 K and μ_C = -6.00 eV/atom (see figure 4), the difference is quite clear, with about 40% C adsorbed on, or dissolved in, the disordered cluster and about 15% C atoms, mostly adsorbed on the surface or subsurface sites of the crystalline clusters. The same holds for the runs at μ_C = -5.25 eV/atom. However, a striking difference can be noticed between the two situations. At μ_C = -6.00 eV/atom the mole fraction of inner carbon atoms gently rises during the course of the Monte Carlo run to reach an equilibrium value. At μ_C = -5.25 eV/atom, the number of carbon atoms adsorbed on the cluster surface increases very rapidly at the beginning of the process, then decreases and rises again. During this process the total number of carbon atoms constantly increases. The sharp peak observed in the inner carbon concentration at the beginning of the adsorption process corresponds to the adsorption of individual C atoms on the cluster surface. As soon as the concentration of surface C atoms is large enough, they tend to form chains and then sp^2 structures that detach from the surface, explaining the depletion of C at the surface. At lower chemical potential, this surface concentration threshold is never reached and the C atoms gradually diffuse towards subsurface or bulk interstitial sites.

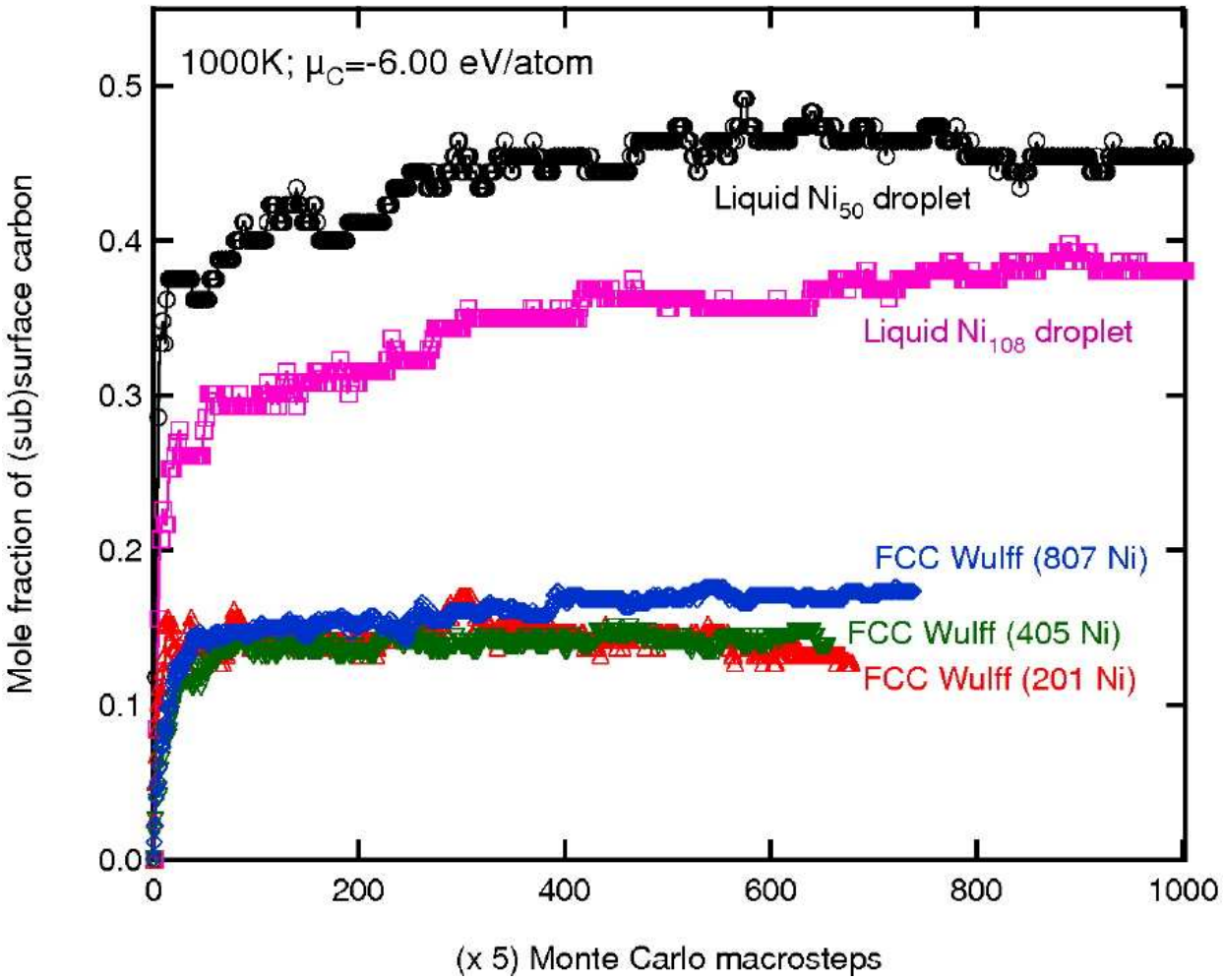

FIG. 4: Mole fractions of surface and subsurface carbon atoms, "inner" carbon atoms in the text, as a function of the number of outer Monte Carlo loops (macrosteps), calculated at 1000 K and μ_C = -6.00 eV/atom. Black circles: Ni_{50} liquid droplet. Pink squares: Ni_{108} liquid droplet. Red up-pointing triangles: fcc 201 Ni cluster. Green down-pointing triangle: fcc 405 Ni cluster. Blue diamond: fcc 807 Ni cluster.

Summarizing this paper, we study the early stages of the formation of carbon nanostructures on small nickel clusters. The GCMC method used enables us to emphasize the critical role of the carbon chemical potential on the resulting structure. We show that an optimal chemical potential value exists to nucleate nanotube caps. Because of the short time scale spanned by the computer simulations as compared to the hundreds of seconds of the experiments, the cap structures obtained are much more defective than what is assumed

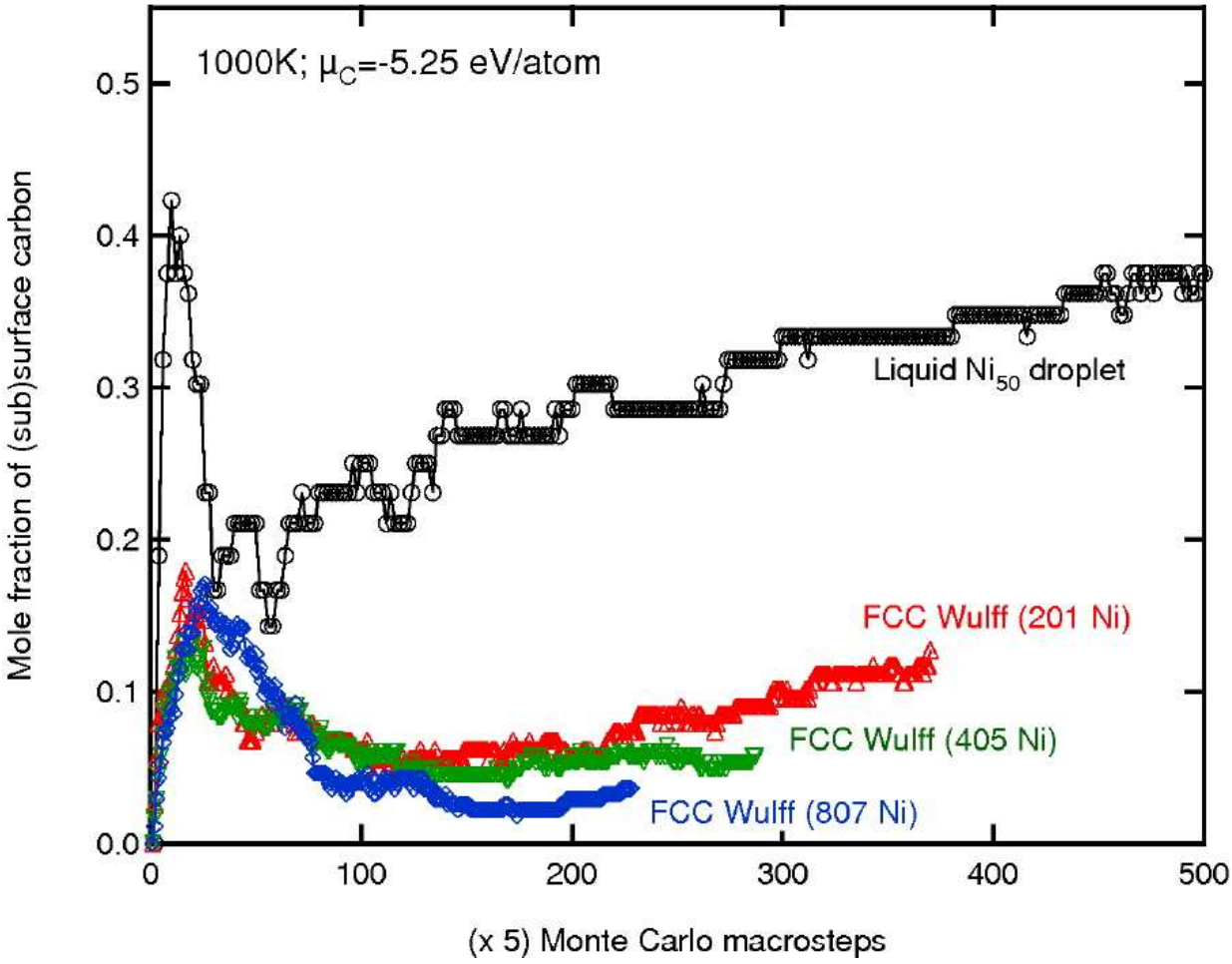

FIG. 5: Mole fractions of surface and subsurface carbon atoms, "inner" carbon atoms in the text, as a function of the number of outer Monte Carlo loops (macrosteps), calculated at 1000 K and μ_C = -5.25 eV/atom. Black circles: Ni_{50} liquid droplet. Red up-pointing triangles: fcc 201 Ni cluster. Green down-pointing triangle: fcc 405 Ni cluster. Blue diamond: fcc 807 Ni cluster.

for the experimental ones. The coarse sampling of the chemical potential values by steps of 0.75 eV/atom also plays a role: less defective caps could probably be grown with μ_C closer to -6.00 eV/atom, but this would require longer simulation times. Under suitable carbon chemical potential and temperature conditions, the early stages of the growth are quite similar to what has been observed on flat surfaces,[20] with the difference that the curvature is imposed by the catalyst particle's size at the moment of the nucleation. The atomistic growth mechanism is more or less in agreement with most of the previous computer simulation studies.[14,15,16,19] However these authors do not take into account the

carbon chemical potential that plays a critical role on the outer nanostructure formed, but also on the surface state of the catalyst. In addition, we show that the presence of carbon in surface, or interstitial subsurface or bulk sites depends on a second parameter that is the structure of the catalyst particle. As in the case of the bulk phase diagram that exhibits a low solubility of carbon in crystalline nickel, but a larger one in the liquid phase, we show that the carbon solubility is larger in disordered clusters. Our study is not yet complete since we should compare liquid and solid structures with the same number of atoms. This work is in progress. However, this is an important finding because the surface state of the catalyst is of fundamental importance if one wishes to understand the origin of the chiral selectivity that has been reported for instance by Bachilo *et al.*.[3]

Acknowledgments

Part of this work is supported by the Belgian Program on Interuniversity Attraction Poles (PAI6) on "Quantum Effects in Clusters and Nanowires". H. A. acknowledges the use of the Interuniversity Namur Scientific Computing Facility (Namur-ISCF), a common project between FNRS, SUN Microsystems, and Les Facultés Universitaires Notre-Dame de la Paix (FUNDP) and the LEMAITRE computer of UCL.

---

[1] *Carbon Nanotubes: Synthesis, Structure, Properties and Applications*, edited by M. S. Dresselhaus, G. Dresselhaus, and P. Avouris (Springer, Berlin, 2001).

[2] A. G. Nasibulin, P. V. Pikhitsa, and Hua Jiang, E. I. Kauppinen, Carbon **43**, 2251–2257 (2005).

[3] S.M. Bachilo, L. Balzano, J. E. Herrera, F. Pompeo, D. E. Resasco, and R. B. Weisman, J. Am. Chem. Soc., **125**, 11186–7 (2003).

[4] S. Reich, L. Li, and J. Robertson, Chem. Phys. Lett. **421**, 469–72 (2006).

[5] G. Lolli, L. Zhang, L. Balzano, N. Sakulchaicharoen, Y. Tan, and D. E. Resasco, J. Phys. Chem. B, **110**, 2108–2115 (2006).

[6] S. Helveg, C. Lopez-Cartes, J. Sehested, P. L. Hansen, B. S. Clausen, J. R. Rostrup-Nielsen, F. Abild-Pedersen, and J. K. Nørskov, Nature, **427**, 6973, 426–9 (2004).

[7] H. Zhu, K. Suenaga, A. Hashimoto, K. Urita, K. Hata, and S. Iijima, Small **1**, 12, 1180–3 (2005).

[8] S. Hofmann, R. Sharma, C. Ducati, G. Du, C. Mattevi, C. Cepek, M. Cantoro, S. Pisana, A. Parvez, F. Cervantes-Sodi, A. C. Ferrari, R. Dunin-Borkowski, S. Lizzit, L. Petaccia, A. Goldoni, and J. Robertson, Nano Letters, **7**, 602–8 (2007).

[9] M. Lin, J. Pei Ying Tan, C. Boothroyd, Kian Ping Loh, Eng Soon Tok, and Yong-Lim Foo, Nano Letters, **6**, 449–52 (2006).

[10] X. Fan, R. Buczko, A. A. Puretzky, D. B. Geohegan, J.Y. Howe, S.T. Pantelides, and S. J. Pennycook, Phys. Rev. Lett. **90**, 145501 (2003).

[11] S. Hofmann, G. Csanyi, A. C. Ferrari, M. C. Payne, and J. Robertson, Phys. Rev. Lett. **95**, 036101 (2005).

[12] F. Abild-Pedersen, J. K. Norskov, J. R. Rostrup-Nielsen, J. Sehested, and S. Helveg, Phys. Rev. B **73**, 115419 (2006)

[13] J. Gavillet, A. Loiseau, C. Journet, F. Willaime, F. Ducastelle, and J.-Ch. Charlier, Phys. Rev. Lett. **87**, 275504 (2001).

[14] J. Y. Raty, F. Gygi, and G. Galli, Phys. Rev. Lett. **95**, 096103 (2005).

[15] F. Ding and K. Bolton, Nanotechnology **17**, 543–8 (2006).

[16] F. Ding and K. Bolton, and A. Rosén, J. Phys. Chem. B **121**, 2775 (2004); Chem. Phys. Lett. **393**, 309 (2004); J. Chem. Phys. **121**, 2775 (2004).

[17] Y. Shibuta and S. Maruyama, Chem. Phys. Lett. **382**, 381 (2003).

[18] Q.-M. Zhang, J. C. Wells, X. G. Gong, and Z. Zhang, Phys. Rev. B **69**, 205413 (2004).

[19] J. Zhao, A. Martinez-Limia, and P. B. Balbuena, Nanotechnology **16**, S575–81 (2005).

[20] H. Amara, Ch. Bichara, and F. Ducastelle, Phys. Rev. B **73**, 11304(2006).

[21] H. Amara, Thèse de Doctorat, Univ. Paris VI (2005); available at `http://lem.onera.fr/Theses.html`.

[22] *The Recursion Method and Its Applications*, R. Haydock ed., Springer Series in Solid State Sciences, **58** (1984); see also the contributions to Solid State Physics **35** (1980).

[23] D. Frenkel and B. Smit, *Understanding Computer Simulation*, (Academic Press, London, 1996).

[24] W. Vervisch, C. Mottet, and J. Goniakowski, Phys. Rev B **65**, 245411 (2002).

[25] G. Brinkmann, P. W. Fowler, and D. E. Manolopoulos, A. H. R. Palser, Chem. Phys. Lett. **315**, 335–47 (1999).